The statistical impact of experimental result scatter of asphalt mixtures on their numerical modelling

Cezary Szydłowski[*]*, Jarosław Górski, Marcin Stienss, Łukasz Smakosz*

Faculty of Civil and Environmental Engineering, Gdansk University of Technology,
Narutowicza 11/12, 80-233 Gdansk, Poland

Abstract. The paper presents selected test results of asphalt mixture conducted in low temperatures. The obtained parameters are highly diverse. It concerns ultimate breaking loads, stiffness parameters related to Young's modulus but also the fracture course. Statistical analysis upon the results makes it possible to relevantly estimate the material-defining parameter values. Such a random approach leads to the mean values of breaking and fracture-triggering loads, dealing with their dispersion too. The estimated parameters allow to form appropriate numerical models of asphalt mixture specimens. This type of analysis supports the laboratory tests. The paper presents the authors' simplified model considering non-uniform material features. The results reflect the scatter of real laboratory test outcomes. In order to do so an algorithm to calibrate the numerical model parameters was created.

1 Introduction

The asphalt mixtures are constantly modified due to strength parameters, abrasive resistance, durability and others. One of the key factors is their resistance to cracking, especially at low temperatures. The conducted laboratory research focused on optimal mixture recipes leading to improved fracture parameters, e.g. stress intensity factors K_{IC} [1, 2, 3]. This issue still seems underrated in design routines. One of the main obstacles to capture the fracture parameters is the scatter of laboratory results. This dispersion is observable at every analytical stage, e.g. ultimate breaking forces for specimens, stiffness based on load-displacement curves, and shapes of the curves. The preparation and the course of tests has a strong influence on the results. The parameters are affected by specimen shape and dimensions, preparation, the mode of loading and deflection measurement. The decisive issue in fracture problem domain is loading control. Observing the CMOD (crack mouth opening displacement) the unloading course is obtained, to relevantly assess the fracture energy.

The scatter of laboratory results should be considered while assessing almost all material parameters. The comprehensive result presentation should take mean values and standard deviations into account, complemented by other statistical parameters. This is the way to properly assess the reliability of asphalt mixtures, in the light of their optimal design. This is a challenging attempt, requiring complex, well-planned research action.

Numerical analysis is one of the essential tools supporting laboratory testing. The finite element method (FEM) modelling of a material structure may be performed on various levels, e.g. mesoscale, multiscale, continuum approaches and others [4 – 12]. The computational power makes it possible to precisely reflect the asphalt mixtures including three-dimensional models. However it is a considerable task to get laboratory-based material parameters of all asphalt mix ingredients, keeping in mind a highly complicated bitumen-aggregate contact definition. Application of these models is limited while specimens are investigated instead of real pavement sections.

A more advantageous variant tends to simplify the numerical model. In this case the asphalt mixture should be homogenized in order to estimate smeared material parameters, to further define simple, homogenized, continuum models. The lowest heterogeneous material volume (RVE) is investigated to reflect global material features [4, 13 – 18]. However, these homogenized numerical models make it difficult to capture the scatter of material parameters [4, 10, 14, 15, 19, 20 – 23].

The purpose of the article is to take into account the heterogeneity of material in numerical modelling. The paper is aimed to define a quasi-continuum numerical model in which the variability of material characteristics will be taken into account. The dispersion of material parameters are considered on the level of finite element generation. The homogenized parameters are assigned on the basis of numerical reflection of laboratory tests. The model is primarily bound to map the fracture process with the aim to estimate the stress intensity factors K_{IC}. In order to do so standard material models of ABAQUS software were employed.

The author's concept to generate the disperse material parameters was proposed here. This approach may be

[*] Corresponding author: cezary.szydlowski@pg.edu.pl

called a Monte Carlo simulation-based constitutive model.

2 Laboratory tests

The research laboratory at the Road Construction Division at the Faculty of Civil and Environmental Engineering, Gdańsk University of Technology conducts experiments to estimate fracture parameters of a mineral-asphaltic mix [19]. The semi-circular test specimens subjected to three-point bending (Fig. 1 and 2) are used. The original test methodology described by the standard EN 12697-44 was appropriately modified. Vertical deflection d and force F were measured. The displacement rate was 1 mm/min. Specimen and loading frame during the test were located in thermostatic chamber of the press to achieve a constant desired test temperature −20°C.

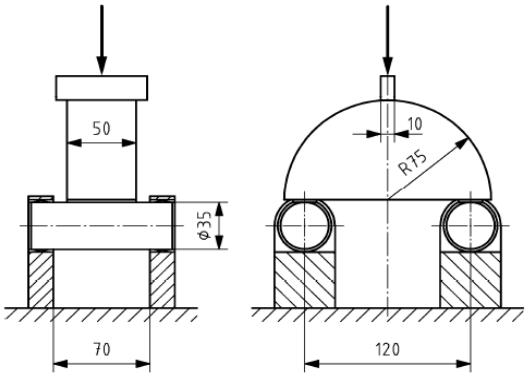

Fig. 1. Semi-circular test specimens subjected to three-point bending

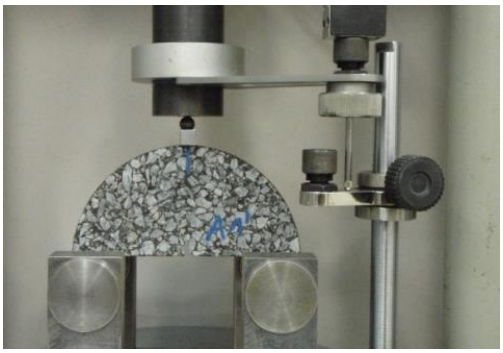

Fig. 2. Semi-circular test specimens subjected to three-point bending, testing jig

The tests were performed with three notch depths, i.e. a =10 mm, 20 mm, 30 mm and on two types of asphalt mixtures for wearing course, i.e. stone matrix asphalt SMA 8 (Fig. 3, Table 1) and porous asphalt PA 8 (Fig. 4, Table 2). The aggregate skeleton was designed according to the Polish Technical Guidelines WT-2 2010 [24].

Four samples were tested in each case. Summary of the laboratory test results are shown in Tables 3-6. Figures 5 and 6 present load F vs. deflection d curves for all tested samples with 20 mm notches.

The results in Tables 3-6 show high dispersion in maximum forces F in the experiment and the linear part slope of the force–deflection (F – d) diagram, to be observed in Figures 5 and 6 (Tan α). It is reflected in standard deviations (SD) and coefficients of variation (CV).

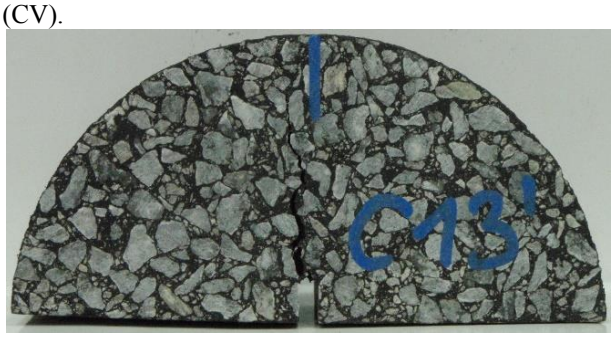

Fig. 3. Stone matrix asphalt SMA 8

Fig. 4. Porous asphalt PA 8

Table 1. Composition of tested asphalt mixtures, SMA 8

SMA 8	Sieve # [mm]	Passes [%]
Aggregate	11.2	100.0
	8	94.2
	5.6	41.2
	2	25.6
	0.125	11.9
	0.063	9.7
	type of aggregate	gneiss, granodiorite and limestone
Bitumen	optimum content [%]	7.0
	type of bitumen	PmB 45/80-55

Table 2. Composition of tested asphalt mixtures – PA 8

PA 8	Sieve # [mm]	Passes [%]
Aggregate	11.2	100.0
	8	91.2
	5.6	13.4
	2	6.7
	0.125	4.8
	0.063	4.1
	type of aggregate	gneiss, granodiorite and limestone
Bitumen	optimum content [%]	6.5
	type of bitumen	PmB 45/80-65

For example, in case of mixture PA 8 and a 20 mm notch result in the maximum force vary from 2700 N to 3280 N (coefficient of variation equal 0.08), and the linear slope of the diagram, representing the specimen stiffness, from 9740 N/mm to 13305 N/mm (coefficient

of variation equal 0.13). The entirety of experiments results in the envelopes of $F - d$ curves varying in the range of 1.5 standard deviation.

Table 3. SMA 8 - fracture toughness, F_{max}

a [mm]	F_{max} [N]			
	sample	mean	SD	CV [%]
10	11881	10870	892	8
	9939			
	11326			
	10333			
20	7939	7110	569	8
	6851			
	6990			
	6659			
30	5423	5264	153	3
	5099			
	5173			
	5362			

Table 4. PA 8 - fracture toughness, F_{max}

a [mm]	F_{max} [N]			
	sample	mean	SD	CV [%]
10	4894	5220	462	9
	5550			
	5678			
	4756			
20	3280	2968	241	8
	2700			
	2902			
	2988			
30	807	1517	475	31
	1741			
	1816			
	1703			

Table 5. SMA 8 - fracture toughness, Tanα

a [mm]	Tanα [N/mm]			
	sample	mean	SD	CV [%]
10	26037	44514	18111	41
	41200			
	41371			
	69449			
20	33015	37782	7084	19
	48086			
	36794			
	33233			
30	28890	27254	2687	10
	30099			
	24365			
	25660			

Table 6. PA 8 - fracture toughness, Tanα

a [mm]	Tanα [N/mm]			
	sample	mean	SD	CV [%]
10	26037	23396	5933	25
	41200			
	41371			
	69449			
20	33015	11857	1593	13
	48086			
	36794			
	33233			
30	28890	8154	2658	33
	30099			
	24365			
	25660			

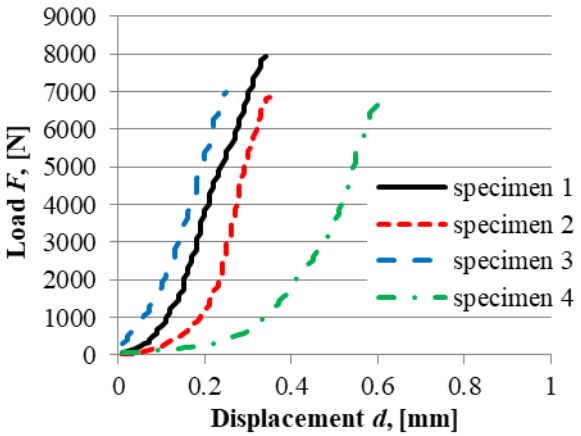

Fig. 5. Laboratory test results for notch depth 20 mm, SMA 8

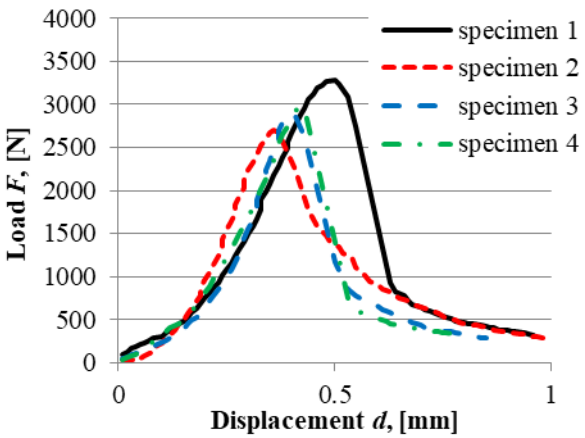

Fig. 6. Laboratory test results for notch depth 20 mm, PA 8

3 Material Monte Carlo model

All computations were performed by ABAQUS software package [25], applying standard material models only.

The featured problem was to reflect the fracture of asphalt mixture specimens while all material parameters are considered random. Thus the Finite Element Method (FEM) model is bound to capture three basic mixture ingredients: aggregate, bitumen mortar and air voids. However, the numerical model does not map a real specimen, made of aggregate linked with bitumen mortar

and voids, due to a prescribed recipe. These three components are homogenized instead on the level of distinct finite elements. The ingredient proportion is bound to make the mechanical specimen response match the laboratory results. The mapping is correct if numerical values lie within the domain of scattered laboratory results.

Thus a numerical experiment was initiated leading to material mixture proportions bringing the global parameters corresponding to the laboratory results. The FEM model was built of an axially compressed cube in plane stress. The boundary conditions were imposed by contact elements leaving the loaded face free to deflect (Fig. 7) The author's software made it possible to generate material parameters of every single finite element. Every material is assumed linear given a relevant Young's modulus. The air voids show their Young's modulus tending to zero. The following material data were assumed: Young's modulus of aggregate E_{ag} = 80000 MPa (constant), Young's modulus of bituminous mortar E_m = 800 MPa, 80 MPa. The ingredient proportions lead the global Young's modulus to the range of appropriate laboratory results. The analytical example is presented in Table 7.

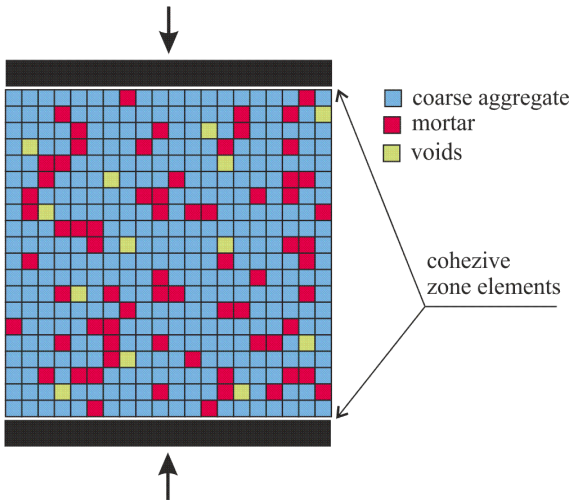

Fig. 7. Samples of generated aggregate dispersions

Table 7. Global E calculation with regard to various percentage of aggregate content

N	% of aggregate	E_m= 800 MPa	E_m= 80 MPa
0	100	80000	80000
1	95	69860	69200
2	90	60980	59990
3	85	44230	38850
4	80	33420	28680
5	75	24930	17510
6	70	17550	10700
7	65	8397	2469
8	60	7184	1647
9	55	4566	766
10	50	2004	413

In order to provide further analysis the following parameters were assumed: E_{ag} = 80000 MPa, 60% of aggregate content, E_m = 80 MPa. A number of 20 distributions was generated, the result was Young's modulus mean value E =1802 MPa, and standard deviations E =225 MPa. The selected stress distributions are shown in Fig. 8. High diversity of outcomes is observed due to random location of finite elements reflecting the aggregate. This approach is not bound to map the material well, it only covers its averaged parameters in order to make the material mechanical response converge the laboratory test results. This is why the proposed approach may be called a Monte Carlo simulation-based constitutive model.

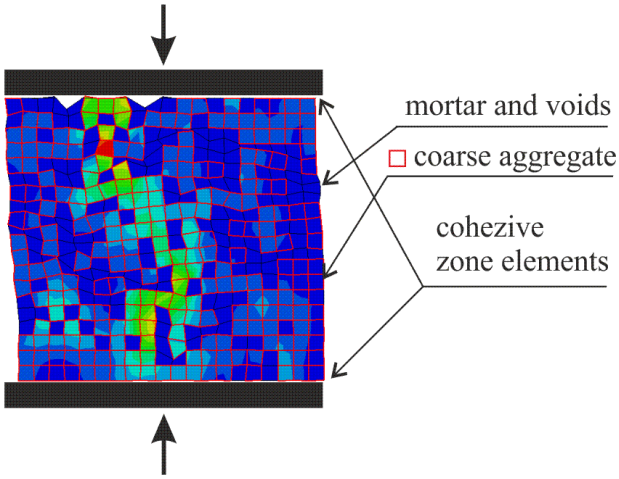

Fig. 8. Samples of generated aggregate dispersions - stress fields under uniform compression

4 FEM calculations

The work is limited to numerical imaging of asphalt mixture specimen fracture. The ABAQUS software employs a number of material models to deal with this feature. The most popular ones are smeared cracks and cohesive connections. Both consider material softening while exceeding extreme stresses (Fig. 9).

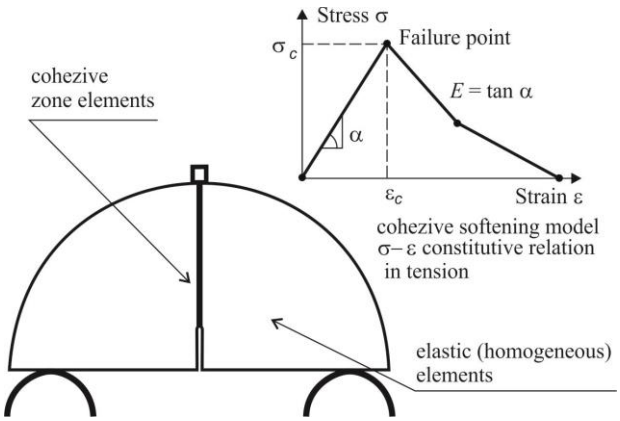

Fig. 9. Cohesive element crack model

The cohesive elements applied allow to trace the crack propagation. Thus it is suggested to predict the direction of crack growth prior to computations. This attempt is appropriate in the case of notched specimens

(Figs 9, 10 and 11). The cohesive elements may be located at the interfaces of all finite elements, but this approach takes advanced model studies. The required material parameters may be taken from laboratory tests. Brittle materials, like asphalt mixtures at low temperatures, may be assumed a brittle-elastic model.

Similarly to the other finite elements the cohesive element characteristics make it possible to randomize the fracture-governing material parameters. The laboratory assessment of tensile parameters taken separately for aggregate and bitumen mortar is a more demanding task. The preliminary surveys point out various tensile and compressive Young's moduli here.

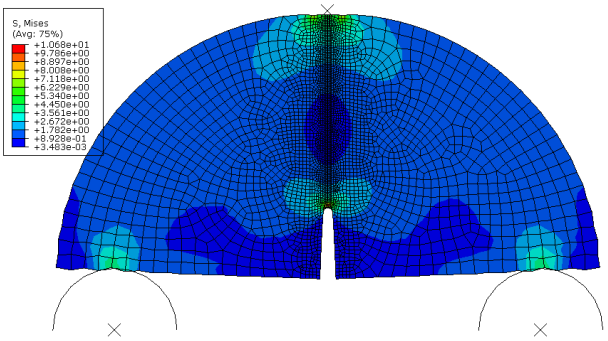

Fig. 10. Sample mesh

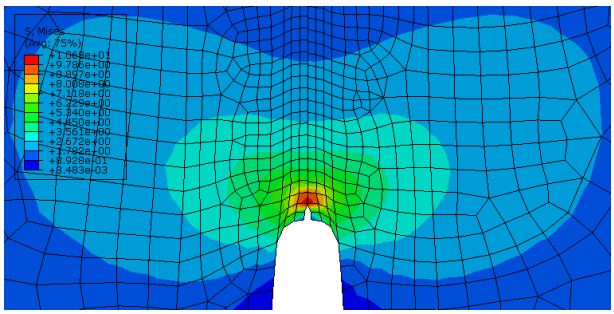

Fig. 11. Cohesive element crack model - propagation of crack

The paper presents the computations of a chosen asphalt mixture PA8 in plane stress state. Three notch depths of 10, 20 and 30 mm are analysed here, to capture the scale effect, essential in such a numerical analysis. U-shaped notch were implemented, witch 3 mm width.

Firstly, the 20 mm specimen notch was considered. A homogeneous material model was assumed of $E = 1$ GPa, $\nu = 0.2$. The elastic material parameter E may be determined implicitly based on the results in Table 4 and 6. These are the three-point bending stiffness values, a product of Young's modulus E and the cross-sectional moment of inertia I. However, the dimension ratio suggests the plane stress pattern instead of a bar model. Because of that the Young modulus value was fixed by trial-and-error method (Fig. 12).

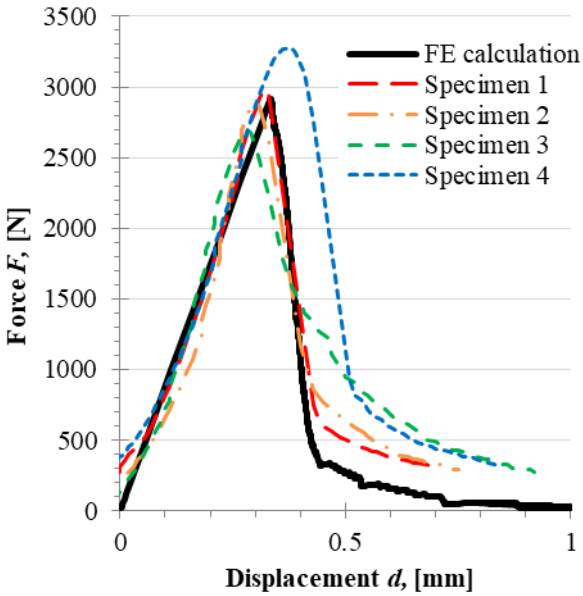

Fig. 12. Comparison of experimental results and FE calculations – diagram *F-d* for the PA 8 asphalt mixture, 20 mm notches

The cohesive element parameters are as follows: traction separation behaviour $K_{nn} = K_{ss} = K_{tt} = 10^{-19}$, total plastic displacement equals 0.0001 and damage stabilization (viscosity coefficient) 0.0001. The elastic material parameter values were based on available laboratory tests but the cohesive parameters were assessed by the trial-and-error attempt. This procedure led to satisfactory results due to a 20 mm specimen (Fig. 12).

The same parameters were applied to the analysis of 10 and 30 mm notch specimens. The discrepancies between the laboratory and FEM results are visible (Fig. 13). But taking into account the dispersion of the laboratory results the diagram are in the allowable range.

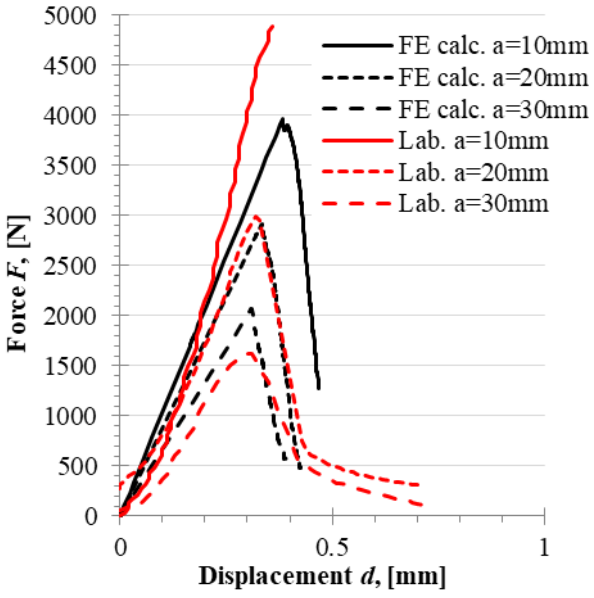

Fig. 13. Comparison of experimental results and FE calculations – diagram *F-d* for the PA 8 asphalt mixture

5 Conclusions

The paper includes preliminary modelling results for asphalt mixture specimens.

The scatter of material parameters was confirmed by laboratory tests, thus considered in the computations.

Deterministic approach to modelling is inappropriate, the variability of material characteristics should be taken into account.

A simple model was created, easy to use in engineering applications.

The material parameters were based on laboratory tests, in the case of cohesive element modelling they were assessed by trial-and-error attempts.

The assumed parameters considering dispersion relevantly take into account the fracture phenomenon of notched test specimens (scale effect).

References

1. T. L. Anderson, *Fracture mechanics fundamentals and applications* (Taylor & Francis, 2005).
2. Y. R. Kim, *Modelling of asphalt concrete* (ASCE Press Mc GrawHil, 2009).
3. L. Wang, *Mechanics of asphalt Microstructure and micromechanics* (ASCE Press Mc GrawHil, 2011).
4. J. Wimmer, B. Stier, J.W. Simon and S. Reese, FINITE ELEM ANAL DES **110**, pp. 43–57 (2016).
5. H. Wang, J. Wang, J. Chen, ENG FRACT MECH **132**, pp. 104–119 (2014).
6. T. You, R. K. A. Al-Rub, M. K. Darabi, E. A. Masad and D. N. Little, CONSTR BUILD MATER **28**, pp. 531–548 (2012).
7. K. H. Moon, A. C. Falchetto and J. W. Hu, CONSTR BUILD MATER **53,** pp. 568–583 (2014).
8. E. Mahmoud, S. Saadeh, H. Hakimelahi and J. Harvey, ROAD MATER PAVEMENT **15(1)**, pp. 153-166 (2013).
9. A. Yin, X. Yang, S. Yang and W. Jiang, ENG FRACT MECH **78**, pp. 2414-2428 (2011).
10. T. Schüler, R. Jänicke and H. Steeb, CONSTR BUILD MATER **109**, pp. 96-108 (2016).
11. X. Li and M. O. Marasteanu, INT J FRACTURE **136**, pp. 285–308 (2005).
12. P. Mackiewicz, J, MATER CIVIL ENG **25(1)**, pp. 140-147 (2013).
13. M. Galouei, A. Fakhimi, COMPUT GEOTECH **65**, pp. 126–135 (2015).
14. T. Kanit, S. Forest, I. Galliet, V. Mounoury, D. Jeulin, INT J SOLIDS STRUCT **40**, pp. 3647–3679 (2003).
15. M. Ostoja-Starzewski, PROBABILIST ENG MECH **21**, pp. 112‑132 (2006).
16. T. Pellinen, E. Huuskonen-Snicker, P. Eskelinen, P. O. Martinez, Journal of traffic and transportation engineering **2(1)**, pp. 30-39 (2015).
17. R. Velasquez, A. Zofka, M. Mugerel, M. O. Marasteanu, INT J PAVEMENT ENG **12:5**, pp. 461-474 (2009).
18. A. Zofka, M. Marasteanu, M. Turos, ROAD MATER PAVEMENT **9:1**, pp. 269-285 (2008).
19. C. Szydłowski, J. Judycki, Highway Engineering **10**, pp. 348–353 (2015) (in Polish).
20. S.-J. Lee, G. Zi, S. Mun, J. S. Kong, J.-H. Choi, ENG FRACT MECH **141**, pp. 212–229 (2015).
21. A. Yin, X. Yang, H. Gao, H. Zhu, ENG FRACT MECH **92**, pp. 40–55 (2012).
22. X. F. Wang, Z. J. Yang, J. R. Yates, A. P. Jivkov, C. Zhang, CONSTR BUILD MATER **75** pp. 35–45 (2015).
23. X. Wang, Z. Yang, A. P. Jivkov, CONSTR BUILD MATER **80**, pp. 262–272 (2015).
24. WT:2-2010. Technical Guidelines, Asphalt Pavements on State Roads, Asphalt Mixes. General Directorate for National Roads and Motorways, 2010. Warsaw, Poland. (in Polish).
25. ABAQUS. ABAQUS analysis user's manual, Habbit, Karlsson & Sorenson Inc. 2010.